

STUDY OF NANO-SiC ADDED MgB₂ SYNTHESIZED BY USING HIGHER BORIDE PHASE AS A PRECURSOR

K. L. Tan*, K. Y. Tan, S. A. Halim, K. P. Lim and S. K. Chen

*Superconductor and Thin Films Laboratory, Physics Department, Faculty of Science,
Universiti Putra Malaysia, 43400 Serdang, Selangor*

**Corresponding author: kimlee.tkl@gmail.com*

ABSTRACT

Both pure and nano-SiC added MgB₂ were prepared by reaction of higher boride phase (MgB₄) and Mg in a two-step sintering method. The first step involved a high temperature (1050 °C) synthesis of MgB₄. However, this reaction gave rise to significant amount of MgO. Hence, acid treatment was done in order to remove MgO while retaining MgB₄ as dominant phase. The second step was followed by the introduction of an appropriate amount of Mg into the acid washed MgB₄ powders to form MgB₂ at a lower sintering temperature (750 °C). Nano-SiC was added according to 2 wt%, 5 wt% and 10 wt% respectively. Both pure and added samples show MgB₂ as a dominant phase. The added samples show other minor phases of Mg₂Si, MgO, MgB₄ and some unreacted SiC was also found. The Scanning Electron Micrographs revealed the well defined hexagonal shape of MgB₂ grains and the microstructure is denser with reduced porosity as compared to the *in-situ* reaction of (Mg + B) samples. The density was found to increase upon increasing the SiC addition level. The superconducting properties were studied and reported as well. The MgB₂ added with 2 wt% SiC has the highest transition temperature of 37K while MgB₂ with 5 wt% SiC exhibits the highest J_c value at 5K at the applied field of 5T among all the added samples.

Keywords: MgB₂; MgB₄; Nano-SiC; Acid Treatment; Superconducting properties;

INTRODUCTION

A superconductor with the ease of fabrication process, low cost material and high performance having the capability of carrying high current is required for large scale applications [1]. The newly discovered MgB₂ superconductor in 2001 meets these requirements which accompanied by its superior properties such as high T_c of 39K and weak-link free grain boundaries. However, MgB₂ turns out to have a very low critical current density (J_c) at high magnetic fields because of poor grain connectivity and lack of effective pinning centers [2]. Numerous attempts have been done such as improvement in the fabrication process and chemical doping. Among these, SiC is the best dopant for J_c enhancement [3-8]. SiC is a highly stable compound even at high temperature and it becomes highly reactive in the nanoscale [9]. The aim of this work is to synthesize the MgB₂ samples with excess Mg as well as to incorporate nano-SiC during sample synthesis by using the reversible process, where the MgB₂ was formed

from reaction of higher boride phase and precursor Mg powders. Since the boron plane in MgB₂ is responsible for superconductivity, it is desirable for the substitution to take place at the Boron site [10] by doping nano-SiC into MgB₂. By then, the local fluctuations of the superconducting order parameter would be induced [10] and the enhancement of J_c in MgB₂ could be investigated.

EXPERIMENTAL METHOD

Polycrystalline samples were prepared from Magnesium (99.7%, 14-20 μm) and Boron (95-97 %, <1μm), both from Tangshan Wei Hao, China and SiC (99%, 15 nm). In order to prepare a phase pure MgB₂, a stoichiometric ratio of Mg:B=1:4 was mixed and ground through. The MgB₄ pellets were synthesized at 1050 °C for 2 hours in an Ar gas protective atmosphere. The high sintering temperature provoked a significant amount of MgO which is undesirable for the formation of MgB₂. The powders were then underwent an acid treatment to remove MgO and hence a “cleaner” MgB₄ was obtained. Next, precursor Mg powders were added into the MgB₄ to form a phase pure MgB₂ as follow:



This sample is defined as pure sample. Later, MgB₄, Mg and nano-SiC was mixed together and ground before pressing into the pellets. Nano-SiC was varied in 2 wt%, 5 wt% and 10 wt%. The pellets were subjected to heat treatment at 750 °C for 4 hours in an Argon gas flow environment. The phase formation was investigated by the X'Pert Pro Pan Alytical PW 3050 X-ray Diffractometer. Phase identification of the samples was done by using Highscore software in support with the ICDD-PDF-2 database. Rietveld refinement was done to analyze the variation of lattice parameter of MgB₂ upon additions of nano-SiC. By using geometrical method, the density of the samples can be determined and the microstructure was observed by using JEOL JSM-6400 Scanning Electron Microscope. The superconducting property was measured by using SQUID magnetometer (MPMS-XL).

RESULTS AND DISCUSSION

Figure 1 shows the comparison of the XRD pattern of MgB₄ powders before and after acid treatment by using 1M of HNO₃. The MgO peaks were represented by the circles and it is obvious that some of the MgO phases were successfully removed by acid-washed and some were reduced to a lower intensity.

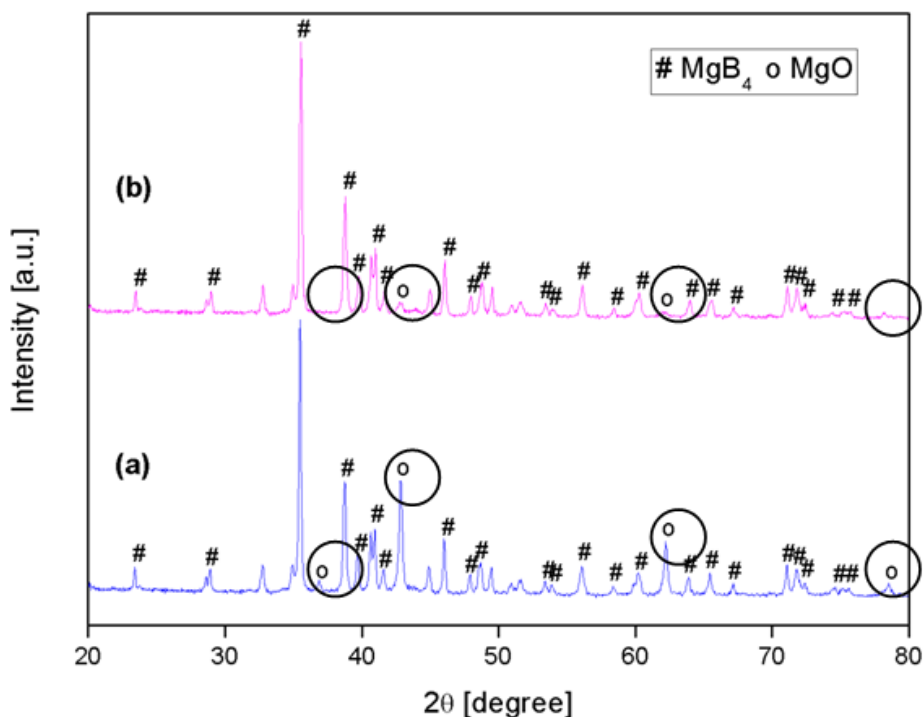


Figure 1: X-ray diffraction of MgB₄ powders (a) before and (b) after acid-washed

Figure 2 shows the x-ray diffraction patterns of pure sample (MgB₄ + Mg), Mg_{1.5}B₂ + 2 wt% SiC, Mg_{1.5}B₂ + 5 wt% SiC and Mg_{1.5}B₂ + 10 wt% SiC samples, each denoted as (a), (b), (c) and (d), respectively. MgB₂ phase remained as the dominant phase with some minor phases of MgB₄, MgO, Mg, Mg₂Si and unreacted SiC. Upon increasing the addition level, the intensity peaks of unreacted SiC was observed to be higher in samples Mg_{1.5}B₂ + 5 wt% SiC and Mg_{1.5}B₂ + 10 wt% SiC, probably due to the saturation of reaction limit of SiC with MgB₂ [8]. Impurity of Mg₂Si was also detected in all the added samples. The increased volume fraction of SiC at higher addition level provokes the reaction between Si from SiC and Mg forming Mg₂Si. It should be noted that the relative intensity Mg₂Si peaks increased simultaneously with the SiC peaks.

S. X. Dou et al. had proposed a mechanism for doping SiC in MgB₂ as explained in the dual reaction model [9]. In this model, two reactions were occurred simultaneously, the first being the reaction between the nano-SiC and Mg to form Mg₂Si as follow:



Concurrently, in the second reaction, the highly reactive C released will be substituted into B sites via the reaction:



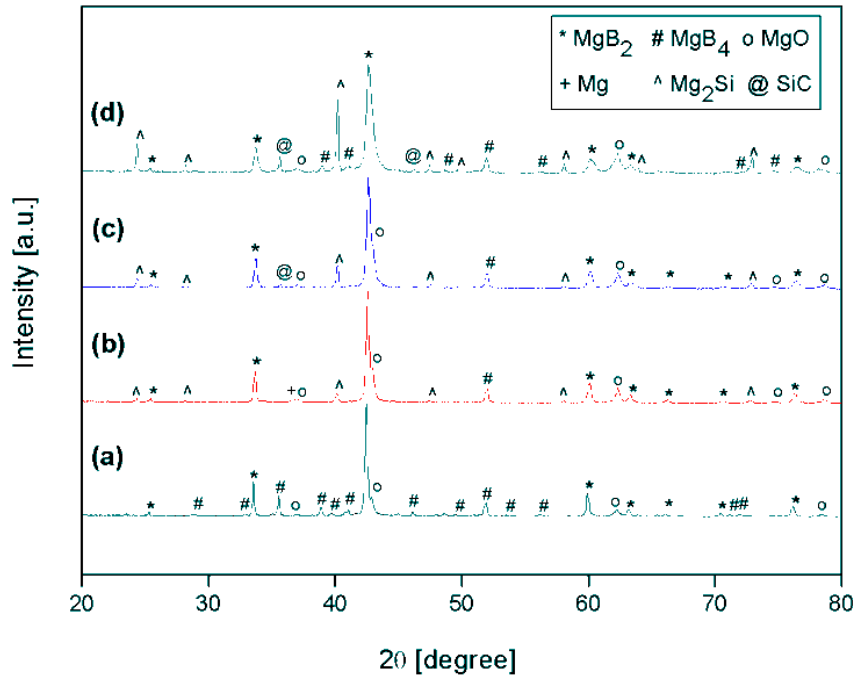


Figure 2: The XRD patterns of pure and SiC added $Mg_{1.5}B_2$ samples sintered at $750^\circ C$ for 4 hours

The lattice parameters obtained from Rietveld refinement are shown in Table 1. Impurities other than MgB_2 peaks were excluded for Rietveld refinement and only the MgB_2 peaks were included for the ease of refinement work. The decrease in a-axis was consistent with other finding on SiC doped MgB_2 [11]. The reaction between Mg and SiC to form Mg_2Si had induced the C to be released and then substituted into the B sites in MgB_2 as shown in equations (2) and (3). Since the C-B bond is located in B plane, the in-plane lattice parameter a was decreased due to the difference in bond length of C-B (1.71 \AA) and C-C (1.78 \AA) [5]. Since the a-axis experiences some changes, it causes the crystal structure of MgB_2 to be distorted. Hence, there is a slight change in c-axis. Another possibility of increased in c-axis may due to the difference in atomic radius between the B and C atoms, in which C has the larger atomic radius of 0.77 \AA over B of 0.46 \AA [11].

Table 1: Samples properties for lattice parameters, superconducting transition temperature and density

Samples	a-axis (\AA)	c-axis (\AA)	T_c (K)	ΔT_c (K)	ρ (g/cm^3)
($MgB_4 + Mg$)	3.0855 (2)	3.5246 (3)	37.2	3.2	1.38
$MgB_2 + 2 \text{ wt\% SiC}$	3.0831 (2)	3.5244 (3)	37.0	5.0	1.47
$MgB_2 + 5 \text{ wt\% SiC}$	3.0803 (4)	3.5253 (6)	36.2	5.2	1.51
$MgB_2 + 10 \text{ wt\% SiC}$	3.0755 (8)	3.5270 (1)	34.8	7.3	1.55

The density of the samples was measured by first obtaining the mass and then dividing it with respect to the volume. The density was found to increase upon increasing addition level and it is more than 50% of the theoretical density. The density obtained from this work is higher than the reported value which is in the range of $1.17\text{-}1.30\text{ g cm}^{-2}$ [12]. Figure 3 shows the microstructure observation indicating the samples obtained from reaction of $(\text{MgB}_4 + \text{Mg})$ have less porosity than the *in-situ* reacted $(\text{Mg} + \text{B})$ samples. S. X. Dou *et al* [12] reported that the SiC doping has no densification effect, independent of doping level due to the high melting point of SiC and it doesn't act as a sintering aid at $800\text{ }^\circ\text{C}$ to $950\text{ }^\circ\text{C}$. The elemental Mg started to evaporate at high temperature and leave a "hole" at the Mg spherical sites (Figure 3). The holes appeared about the size and the shape of precursor Mg powder. Higher J_c could be achieved if the density of the samples is further improved [12].

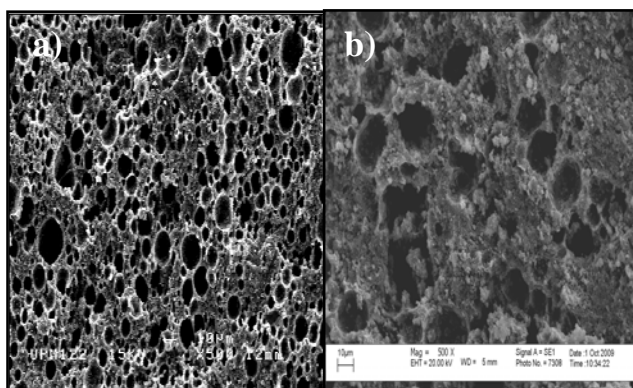


Figure 3: Microstructures of (a) $(\text{Mg} + \text{B})$ sample and (b) $(\text{MgB}_4 + \text{Mg})$ sample sintered at $750\text{ }^\circ\text{C}$. The appearance of porosity is caused by the evaporation of Mg powders

The SEM images of the pure and added samples were shown in Figure 4. The pristine MgB_2 grains are clearly seen except in the pure sample and $\text{MgB}_2 + 10\text{ wt}\%$ SiC samples. The average grain size is about the range of $0.57\text{ }\mu\text{m}$ to $1\text{ }\mu\text{m}$. But the grain size was decreased upon increasing the SiC addition level, hence contributed to more grain boundary, as was also reported by S. X Dou *et al.* [9]. It is expected that some of the grains in the microstructures shown in Figure 4(d) are the remnant of unreacted nano-SiC and Mg_2Si according to the XRD patterns showing that the volume fraction of the two phases increased upon increasing the SiC addition level.

Figure 5 shows the superconducting transition temperature for pure and added samples. The pure sample showed a quite sharp transition temperature with the highest T_c of 37.2 K but the added samples showed a decreased in critical temperature with increasing addition level. One of the root causes is the lower volume fraction of the superconducting phase of MgB_2 since most of the Mg had taken part in reaction with Si to form Mg_2Si . This is consistent with the result from the increased of the breadth of the transition temperature (ΔT_c), which determines the purity level in the samples. It is clear from Figure 5 that the $\text{MgB}_2 + 10\text{ wt}\%$ SiC sample had the highest value of ΔT_c of

7.3K. The other reason for the decrease in T_c is due to the distortion of lattice structure as shown by the change in lattice parameters (Table 1) because of carbon doping.

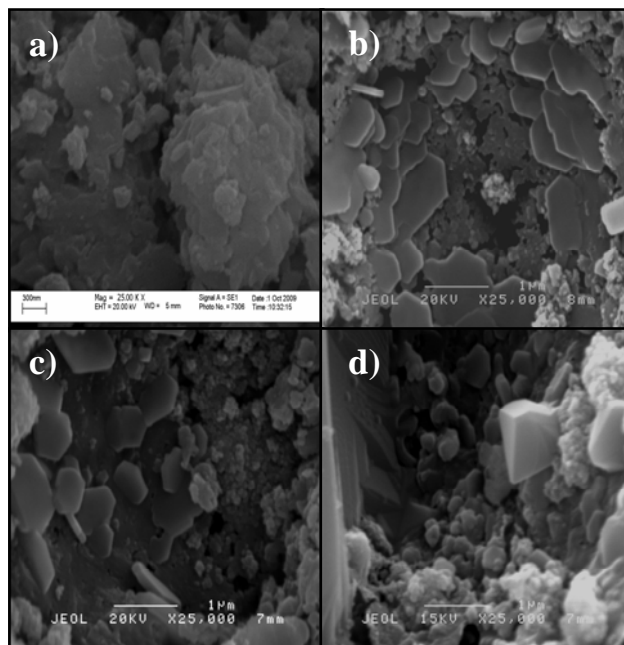


Figure 4: Scanning electron micrographs of (a) pure $Mg_{1.5}B_2$, (b) $Mg_{1.5}B_2 + 2 \text{ wt\% SiC}$, (c) $Mg_{1.5}B_2 + 5 \text{ wt\% SiC}$ and (d) $Mg_{1.5}B_2 + 10 \text{ wt\% SiC}$

The critical current density (J_c) at 5K was obtained from the magnetization hysteresis loops based on the Bean model. Figure 6 shows the normalised J_c decreased monotonically upon increasing the applied field. It was noted that the J_c of pure sample showed a rapid drop as compared to other samples. At lower field, the pure sample showed the highest magnitude of J_c but at higher field, the $Mg_{1.5}B_2 + 5 \text{ wt\% SiC}$ sample exhibited the superior behaviour of J_c among all the samples. The introduction of nano-SiC into the $Mg_{1.5}B_2$ enhanced the behavior of J_c . It is well known that grain boundary pinning is the main mechanism at enhancement of J_c at high fields for MgB_2 [5]. In addition to that, from the dual reaction model, both the reaction of forming Mg_2Si and free C being substituted into MgB_2 helps in pinning of vortices [13]. As far as pinning is concerned, the type of pinning that involved in this work are most probably the grain boundary pinning which is due to the presence of grain boundary precipitates of Mg_2Si and the point defects due to the inclusions of nano-SiC [13]. It is worth noticing that despite the large amount of non-superconducting phase formed, adding MgB_2 with nano-SiC can significantly enhance J_c in high fields with only a slight reduction in T_c [14]. The $MgB_2 + 5 \text{ wt\% SiC}$ sample shows the highest J_c at 5K at the applied field of 5T with only slight drop in T_c by 1K as compared to the pure sample (Table 1).

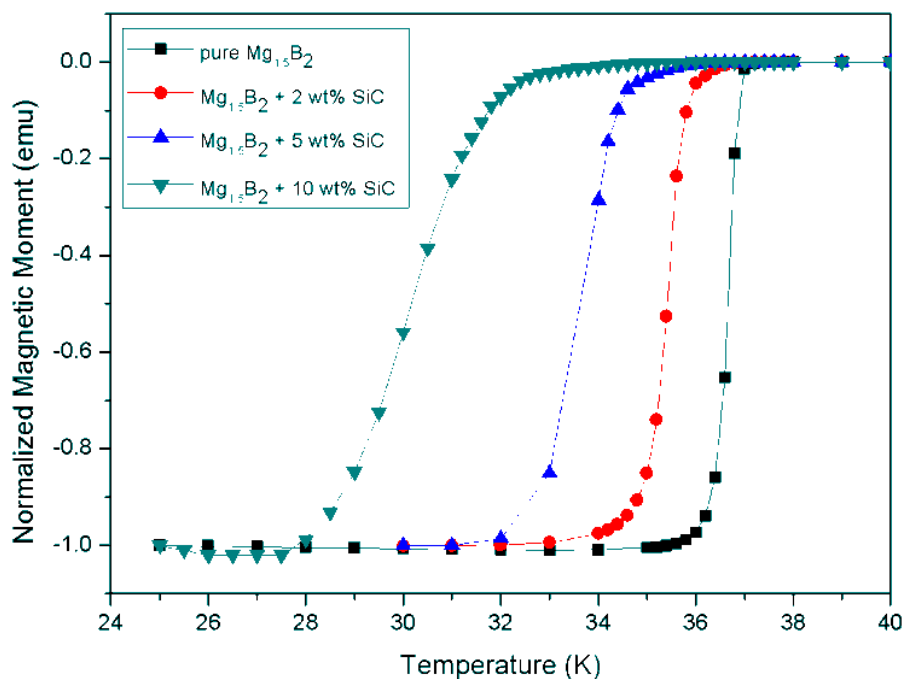


Figure 5: Normalized magnetic moment as a function of temperature for all the samples

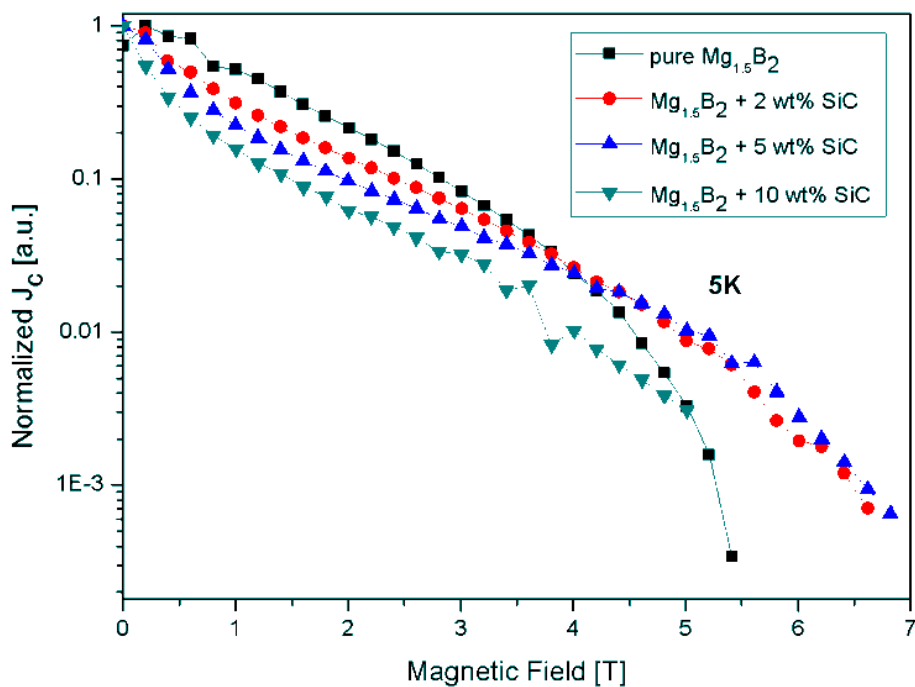


Figure 6: Normalized critical current density versus applied magnetic field, $J_c(H)$ for all the samples at 5K

CONCLUSION

Polycrystalline $Mg_{1.5}B_2$ samples were prepared by reaction between Mg and MgB_4 . Some samples were added with nano-SiC by using the same procedure. The phase formation showed that MgB_2 appeared as the parent phase with some minority phases of MgB_4 , MgO, Mg, Mg_2Si and remnant SiC. Upon increasing the addition level, the a-axis parameter was decreased due to the substitution of C in the B sites and this slightly distorted the crystal structure of MgB_2 while leaving c-axis slightly increased. The density was found to increase upon increasing the addition level and samples obtained from reaction of ($MgB_4 + Mg$) have less porosity than the *in-situ* reacted (Mg + B) samples. Microstructures analysis showed the hexagonal MgB_2 grain shape with the size in the range of about 0.57 μm to 1 μm . The pure sample showed a sharp transition T_c and the T_c was decreased upon increasing the addition level due to the increased of non-superconducting phase formed and C doping into B site. In order to study the pinning effect, the graph of normalized J_c showed the $MgB_2 + 5$ wt% SiC sample had the highest J_c at 5K at the applied field of 5T. This is most probably due to the grain boundary pinning and the pinning of point defects which occurred by adding nano-SiC added into MgB_2 sample.

ACKNOWLEDGMENT

This work is being supported by the Ministry of Science, Technology and Innovation Malaysia (MOSTI) under ScienceFund (contract no. 03-01-04-SF0920).

REFERENCES

- [1] Larbalestier, D., A. Gurevich, D.M. Feldmann, and A. Polyanskii, *Nature*, **414** (2001) 368-377
- [2] Lim, J.H., J.H. Shim, J.H. Choi, J.H. Park, W. Kim, J. Joo, and C.J. Kim, *Physica C: Superconductivity and its Applications*, **469** (15-20) (2009) 1182-1185
- [3] Yamamoto, A., J. Shimoyama, S. Ueda, Y. Katsura, I. Iwayama, S. Horii, and K. Kishio, *Physica C: Superconductivity and its Applications*, **445-448** (1-2) (2006) 806-810
- [4] Chen, S.K., X. Xu, J.H. Kim, S.X. Dou, and J.L. MacManus-Driscoll, *Superconductor Science and Technology*, **22** (12) (2009) 125005
- [5] Zhang, Y., S.X. Dou, C. Lu, S.H. Zhou, and W.X. Li, *Physical Review B*, **81**(9) (2010) 094501
- [6] S Zhou, A.V.P., Y Zhang and S X Dou, *Journal of Physics: Conference Series*, **97**(1) (2008) 012081
- [7] Ranot, M., S.G. Jung, W.K. Seong, N.H. Lee, W.N. Kang, J. Joo, C.J. Kim, B.H. Jun, and S. Oh, *Physica C: Superconductivity and its Applications* **470** (2010) (Supplement 1) S1000-S1002
- [8] Ding, Y., H.C. Wang, F.X. Zhao, Z.X. Shi, Z.L. Zhang, L. Ma, and H.L. Suo, *Journal of Superconductivity and Novel Magnetism*, **23**(5) (2010) 633-636

- [9] Dou, S.X., O. Shcherbakova, W.K. Yeoh, J.H. Kim, S. Soltanian, X.L. Wang, C. Senatore, R. Flukiger, M. Dhalle, O. Husnjak, and E. Babic, *Physical Review Letters*, **98** (9) (2007) 097002
- [10] Dou, S.X., A.V. Pan, S. Zhou, M. Ionescu, X.L. Wang, J. Horvat, H.K. Liu, and P.R. Munroe, (2003). *Journal of Applied Physics*, **94** (3) 1850-1856
- [11] R. Askeland, D. and P.P. Phule, *The Science and Engineering of Materials Fifth Edition* ed.: (Thomson, 2006) 842
- [12] Dou, S.X., A.V. Pan, S. Zhou, M. Ionescu, H.K. Liu, and P.R. Munroe, *Superconductor Science and Technology*, **15** (11) (2002) 1587-1591
- [13] Arpita Vajpayee, V.P.S.A., G. L. Bhalla and H. Kishan *Nanotechnology*, **19** (12) (2008) 125708
- [14] Dou, S.X., S. Soltanian, W.K. Yeoh, and Y. Zhang, *IEEE Transactions on Applied Superconductivity*, **15** (2 PART III) (2005) 3219-3222